Heart infarct in NOD-SCID mice: Therapeutic vasculogenesis by transplantation of human CD34$^+$ cells and low dose CD34$^+$KDR$^+$ cells

Rosanna Botta,*,[†] Erhe Gao,[‡] Giorgio Stassi,[§] Desirée Bonci,[†] Elvira Pelosi,[†] Donna Zwas,* Mariella Patti,[§] Lucrezia Colonna,[*] Marta Baiocchi,[†] Simona Coppola,[†] Xin Ma,[‡] Gianluigi Condorelli,*,[¶,#] and Cesare Peschle*,[†]

*Kimmel Cancer Center, Thomas Jefferson University, Philadelphia, Pennsylvania, 19107; [†]Department of Hematology, Oncology and Molecular Medicine, Istituto Superiore Sanità, 00161, Rome, Italy; [‡]Center for Translational Medicine, Department of Medicine, Thomas Jefferson University, Philadelphia, Pennsylvania, 19107; [§]Department of Surgical and Oncological Sciences, University of Palermo, Italy; [*]Department of Medicine, Division of Cardiology, Thomas Jefferson University, Philadelphia, Pennsylvania, 19107; [¶]Laboratory of Molecular Cardiology, San Raffaele Science Park of Rome, 00128, Italy; [#]Institute of Molecolar Medicine, University of California, San Diego 92093, La Jolla, California

Corresponding author: Cesare Peschle, M.D., Thomas Jefferson University, Kimmel Cancer Center, Bluemle Life Sciences Bldg., Room #609 - 233, South 10th Street, Philadelphia, PA 19107-5541. E-mail: cesare.peschle@mail.jci.tju.edu

ABSTRACT

Hematopoietic (Hem) and endothelial (End) lineages derive from a common progenitor cell, the hemangioblast: specifically, the human cord blood (CB) CD34$^+$KDR$^+$ cell fraction comprises primitive Hem and End cells, as well as hemangioblasts. In humans, the potential therapeutic role of Hem and End progenitors in ischemic heart disease is subject to intense investigation. Particularly, the contribution of these cells to angiogenesis and cardiomyogenesis in myocardial ischemia is not well established. In our studies, we induced myocardial infarct (MI) in the immunocompromised NOD-SCID mouse model, and monitored the effects of myocardial transplantation of human CB CD34$^+$ cells on cardiac function. Specifically, we compared the therapeutic effect of unseparated CD34$^+$ cells vs. PBS and mononuclear cells (MNCs); moreover, we compared the action of the CD34$^+$KDR$^+$ cell subfraction vs. the CD34$^+$KDR$^-$ subset. CD34$^+$ cells significantly improve cardiac function after MI, as compared with PBS/MNCs. Similar beneficial actions were obtained using a 2-log lower number of CD34$^+$KDR$^+$ cells, while the same number of CD34$^+$KDR$^-$ cells did not have any effects. The beneficial effect of CD34$^+$KDR$^+$ cells may mostly be ascribed to their notable resistance to apoptosis and to their angiogenic action, since cardiomyogenesis was limited. Altogether, our results indicate that, within the CD34$^+$ cell population, the CD34$^+$KDR$^+$ fraction is responsible for the improvement in cardiac hemodynamics and hence represents the candidate active CD34$^+$ cell subset.

Key words: neoangiogenesis • endothelial precursors • hematopoietic stem cells

In the past few years, the possibility of using progenitor/stem cells to cure degenerative diseases has generated great excitement. In fact, the potential applications of cell replacement therapy are numerous. In cardiovascular medicine, myocardial infarction (MI) and heart failure are two disease states in which cell replacement holds therapeutic promises. Experimental evidence in murine models of acute ischemic damage suggested that infusion of bone marrow mononculear (BM MNCs) or endothelial (End) cells expanded there improves myocardial perfusion and viability through angiogenesis (1–6). Following these studies, the use of BM cells for therapeutic application has been extended to small clinical trials. Specifically, autologous cells were injected during primary angioplasty in patients with acute myocardial infarct (MI): an improvement of cardiac function and perfusion was reported in the cohort of patients injected with BM MNCs (7) or peripheral blood (PB) CD34$^+$ hematopoietic (Hem) progenitors (8). These clinical studies assumed that BM MNCs and PB CD34$^+$ cells contain a few End precursors, as previous experimental studies suggested (1, 9). Beside angiogenesis, it has been suggested that BM progenitors may differentiate into cardiomyocytes (CMCs) in vivo. In the mouse, cKit$^+$lin$^-$ cells, when injected in the peripheral area of a MI, were shown to differentiate not only into End cells, contributing to neoangiogenesis, but also into CMCs (10). Similarly, the mobilization of BM progenitors induced by G-CSF and SCF improved myocardial contractility and cardiomyogenesis after MI in rats (11). In another study, the differentiation of BM cells into CMCs has been shown to be a feature of a small set of primitive hematopoietic cells, pertaining to the "side-population" (12).

Using an in vitro coculture assay, we demonstrated that embryonal and perinatal End precursors can be induced to differentiate into CMCs (13). More recently, PB CD34$^+$ progenitors, stimulated with VEGF in vitro to favor their End commitment, were shown to differentiate into CMCs in coculture assays (14).

Whether human CD34$^+$ progenitors can be induced to differentiate in vivo into CMCs is not known yet. Moreover, the relative contribution of CD34$^+$ progenitors to angiogenesis and cardiomyogenesis is not clear. In this manuscript, we describe the effects of human cord blood (CB) CD34$^+$ progenitor cell transplantation after MI in the NOD-SCID mouse model, as evaluated at the hemodynamic level and in terms of neoangiogenesis and neocardiomyogenesis. Since CD34$^+$KDR$^+$ cells are enriched for progenitor/stem cells giving rise to End and/or Hem progeny (15, 16, 17), we also explored the effects induced by transplantation of the CD34$^+$KDR$^+$ subfraction. CB CD34$^+$ cells induce beneficial hemodynamic effects, give rise to angiogenesis, and are responsible for a significant, even if limited, cardiomyogenesis. More important, we show that similar effects can be obtained using a 2-log lower number of CD34$^+$KDR$^+$, but not of CD34$^+$KDR$^-$ cells.

MATERIALS AND METHODS

Progenitor cell purification

Human umbilical cord blood (CB) was obtained from the umbilical vein immediately after normal full-term deliveries with previous informed consent. MNCs were separated from heparinized CB by Ficoll-Hypaque density gradient centrifugation according to standard procedures (Amersham Biosciences AB, Uppsala, Sweden). After red cell removal by lysis with an ammonium chloride solution (StemCell Technologies, Inc., Vancouver, BC), CD34$^+$ cells

were isolated using the MACS magneto-bead separation system (Miltenyi Biotech, Auburn, CA). After two successive fractionation steps, the CD34$^+$ cell fraction had a purity of >95%, as determined by fluorescence-activated cell sorting (FACS) analysis using a CD34-specific monoclonal antibody, anti-HPCA-2 (Becton Dickinson, San Jose, CA).

For KDR$^+$ cell separation, purified CD34$^+$ cells were incubated for 30 min on ice with saturating amounts of biotinylated anti-KDR mAb (Sigma, clone V9134) and anti-CD34 FITC (fluorescein isothiocyanate) mAb. Cells were then washed and labeled with SA-PE (streptavidin-phycoerythrin) antibody (R&D Systems, Minneapolis, MN). After further washing, CD34$^+$KDR$^+$ and CD34$^+$KDR$^-$ subfractions were sorted using a MoFlo cell sorter (Cytomation, Fort Collins, CO; fluorescence emission, 525 and 527 nm). Both sorted fractions were reanalyzed for purity after cell sorting performing a dye exclusion with 7-AAD (7-aminoactinomycin D; Sigma-Aldrich, St. Louis, MO). The purity of the KDR$^+$ cell fraction ranged from 80% to 95% (Fig. 1A).

Serum-free starvation culture

CD34$^+$KDR$^+$ and CD34$^+$KDR$^-$ cells were seeded at low densities in U-shaped wells containing serum-free medium as previously reported (15). The small blastlike cells were counted using Trypan blue dye. VEGF level in the culture medium was assayed using the Chemioluminescent Immunoassay kit (Quantiglo, R&D, Minneapolis, MN).

In vitro coculture experiments

Cells were infected using an HIV-derived vector expressing green fluorescence protein (GFP) (18). Briefly, CD34$^+$ cells were incubated with viral supernatant in 24-well plates at the concentration of 5×10^4 cells/ml in the presence of 4 µg/ml of polybrene without addition of human GFs. Cells were then centrifuged for 45 min at 1800 rpm/32°C, placed in a CO_2 incubator for 2 h, washed and cultured in serum-free medium supplemented with 0.01 ng/ml SCF. In other experiments, differentiation of CD34$^+$ cells was performed without previous lentiviral GFP gene transduction.

After 48 h, GFP expression was verified by FACS analysis. GFP$^+$CD34$^+$ cells were seeded in 24-well plate over a rat neonatal CMC feeder layer at the concentration of 1×10^4 CD34$^+$ cells/ 1×10^5 CMCs using CMC-conditioned medium supplemented with 0.01 ng/ml SCF. Cells were maintained in culture for ~14 days, replacing medium weekly.

In other experiments, CD34$^+$KDR$^+$ and CD34$^+$KDR$^-$ cells (0.3 to 1×10^4 cells) were plated over a rat neonatal CMC feeder layer (1×10^5 cells) in chamber slides (1-cm diameter round wells) to allow confocal analysis at high magnification. Cells were analyzed after 12 days by immunofluorescence as described below.

Myocardial infarction and hemodynamic assessment in mice

Breeding pairs of NOD-SCID mice (originally obtained from Dr. Dominique Bonnet, Corriel Institute, Camden, NJ) were expanded and maintained under pathogen-free conditions in the animal facility of the Kimmel Cancer Institute (Thomas Jefferson University, Philadelphia, PA).

All of the experimental procedures were approved by Thomas Jefferson University's Animal Care and Use Committee.

Seven- to nine-week-old male NOD-SCID mice were anesthetized with isoflurane (2%), the pericardium opened, and a 6.0 silk suture (Ethicon, Inc., Piscataway, NY) placed at the distal 1/3 of the left anterior descending coronary artery (LAD) (Fig. 1B). Cells were then injected into the peri-ischemic area. Cells (2×10^5 $CD34^+$ cells or MNCs; 2×10^3 $CD34^+KDR^+$ or $CD34^+KDR^-$ cells) were injected in 15 µl PBS w/o Ca^{++} or Mg^{++}. After the injection, the heart was immediately placed back into the intrathoracic space, the thorax was closed, and manual evacuation of pneumothoraces was performed. In the sham group, the LAD was left unligated as described (19, 20).

After 21 days, mice were studied for hemodynamic parameters. Briefly, after full anesthesia with intraperitoneal injections of 2.5% Avertin (0.02 ml/g, Sigma-Aldrich), the right carotid artery was exposed. A PE-10 catheter (Millar Instr., Houston, TX) connected to a pressure transducer was inserted retrograde from the carotid artery to the left ventricular cavity. The mean arterial blood pressure (MABP), left ventricular pressure (LVP), left ventricular systolic pressure (LVSP), left ventricular end diastolic pressure (LVEDP), first derivative of the LVP ($+dP/dt_{max}$ and $-dP/dt_{max}$), and heart rate (HR) were measured using computer algorithms and an interactive video graphics program (Po-Ne-Mah Physiology Platform P3 Plus, Gould Instrument Systems, Inc., Valley View, OH). Two groups of mice were analyzed for hemodynamic parameters 5 months after MI and injection.

Quantification of infarct size

Three weeks after LAD ligation and injection, hearts were quickly excised, atria and right ventricular free wall were removed, and the left ventricle (LV) was sliced into 1-mm-thick sections perpendicular to the long axis of the heart; TTC (1% 2,3,5-triphenyltetrazolium chloride; Sigma-Aldrich) staining was performed as described previously (19). Normal myocardium was identified by brick-red coloration and infarcted areas by lack of dehydrogenase activity (white coloration). The circumference of necrotic and viable tissue was measured using SigmaScan Pro 5 (SPSS Inc., Chicago, IL): percent myocardial infarction was calculated as the total length of circumference of infarction area divided by total length of circumference of LV (circumference of infarct + alive tissue). Slices were photographed with a digital camera (1600 × 1200 dpi).

Immunostaining Procedures

Immunohistochemical staining was performed on frozen 5-µm-thick mouse heart sections. Sections, were fixed with 2% paraformaldehyde (PFA) in phosphate buffer (PBS 1×) for 20 min at 37°C and following two washes in PBS for 5 min, were permeabilized with PBS/0.1% Triton X-100 for 3 min at room temperature. After a gentle rinse with PBS, tissue sections were exposed for 1 h, at 37°C, to lectin I (FL-1201, Fluorescein Griffonia Simplicifolia Lectin I, Isolectin B_4, Vector) or WGA, (SP-0090, Fluorescein-labeled Wheat Germ Agglutinin, Vector D.B.A., Segrate, Milan, Italy). After two washes in PBS, sections were incubated for 1 h at 37°C with specific antibodies for human nuclei antigen, HNA (MAB 1281, mouse IgG1, Chemicon International, Inc., Temecula, CA) diluted 1:50 in PBS containing 3% bovine serum albumin

(BSA, Sigma Aldrich, Srl MI), to block unspecific staining, and 0.05% Tween 20. Then, sections were washed in PBS and incubated with Rodamine Red secondary antibody (R-6393, goat anti-mouse IgG (H$^+$L) Molecular Probes Europe BV, PoortGebouw, Leiden, The Netherlands). Nuclei were stained by membrane permeant Hoechst 33342 (Molecular Probes). Slides were mounted using fluorescent mounting medium (S3023 Dako S.p.A, MI). Slides were observed and analyzed by confocal laser-scanning microscopy (Olympus Optical CO, Europa GmbH, Hamburg, Germany). Myocardial apoptosis was detected as described (21).

For coculture experiments, immunofluorescence staining was performed directly in the culture plate or chamber slide. Cells were fixed with 4% paraformaldehyde/PBS for 30 min at 25°C, washed with PBS, and permeabilized for 15 min with PBS, 0.2% Triton X-100, BSA 1% (bovine serum albumin) at room temperature. Cells were incubated overnight at 4°C with the following monoclonal antibodies in PBS, 1% BSA: anti-human nuclei (1:100) plus either anti-Troponin I (mouse IgG2b, kindly given by Prof. S. Ausoni, University of Padova, Italy, 1:3000) or anti-myosin rabbit polyclonal, kindly provided by Prof. G. Cossu, University La Sapienza, Rome, Italy (1:100). After washing, cells were incubated with secondary antibodies for 1 h at room temperature, which included Cy3-conjugated anti-mouse IgG1 (1:300, Caltag, Burlingame, CA) plus either Cy5 conjugated anti-mouse IgG2b (Caltag) or FITC-conjugated anti-rabbit (DAKO), depending on the primary antibody used. Cells were washed three times and stained with the nuclear dye Hoechst 33342 before analysis. Images were collected with a Laser Confocal Scanning Microscope (IX81, Olympus Inc., Melville, NY).

Statistical Methods

All values were expressed as mean ± SEM. Comparison between groups was made with one-way ANOVA. $P < 0.05$ was considered statistically significant.

RESULTS

Resistance of CD34$^+$KDR$^+$ cells to apoptosis in serum-free culture via autocrine VEGF release

Paracrine and autocrine release of VEGF was explored in 48 h liquid suspension serum-free cultures seeded with a large number of CD34$^+$ and CD34$^+$KDR$^-$ cells (5×10^4 cells/0.2 ml) or a 50-fold lower number of CD34$^+$KDR$^+$ cells (10^3/0.2ml) (Table 1). A significant release of VEGF was observed not only in the CD34$^+$KDR$^-$ cultures (41.3±12.6 pg/ml), but also in the control CD34$^+$ (50.0±4.1) and CD34$^+$KDR$^+$ cultures (42.5±9.7): it is apparent, therefore, that an effective autocrine VEGF loop functions in the last group.

To explore the functional role of autocrine VEGF, we seeded CD34$^+$KDR$^+$ cells in serum-free suspension culture at low density (2×10^3 cells/ml) (a representative experiment is shown in Fig. 2): many of the small blastlike cells die, but ~40% of the cells survive for an extensive period of time (left panel). The cell survival seems to be mediated by the autocrine release of VEGF (16 pg/ml of culture medium at day 22), thus in line with results in (22). In the control CD34$^+$KDR$^-$ cultures, all cells rapidly die (right panel).

Altogether, it is apparent that a low number of CD34$^+$KDR$^+$ cells release significant amounts of autocrine VEGF, which renders the cells resistant to apoptosis even in serum-free starvation

culture. Conversely, CD34$^+$KDR$^-$ cells, seeded at the same density, rapidly undergo apoptosis in these same culture conditions.

On this basis, as well as in view of the marked enrichment of CD34$^+$KDR$^+$ cells for primitive Hem-End cells (15, 16, 17), we planned to transplant in the heart infarct area a relatively large number of CD34$^+$ cells (2×10^5/mouse) vs. a 2-log lower number of CD34$^+$KDR$^+$ cells and CD34$^+$KDR$^-$ cells (2×10^3/mouse).

Hemodynamic effects of CD34$^+$, CD34$^+$KDR$^+$, and CD34$^+$KDR$^-$ cell injection

Short-term invasive hemodynamic data

At 3 weeks after coronary artery ligation, transplantation of CB CD34$^+$ improves LV function. Hemodynamic assessment by Millar catheterization demonstrated a significant increase in +dP/dt (a key index of systolic function) and –dP/dt (a key index of diastolic function), as well as a significant drop of LVEDP at 21 days after MI in mice transplanted with 2 × 10^5 CD34$^+$ cells, as compared with mice transplanted with PBS solution ($P<0.05$). Intriguingly, animals transplanted with 2×10^3 CD34$^+$KDR$^+$ cells also showed a significant improvement of these cardiac functional parameters, as compared with those transplanted with 2 × 10^3 CD34$^+$KDR$^-$ cells ($P<0.05$) (Fig. 3). Thus, these experiments demonstrate that not only CD34$^+$, but also CD34$^+$KDR$^+$ cells improve cardiac function when transplanted after MI.

Size of the infarct area

The improvement of cardiac function by in vivo injection of unseparated CD34$^+$ and CD34$^+$KDR$^+$ cells after induction of MI prompted us to determine the effect of these populations on infarct size. TTC analysis performed at 21 days after MI shows a highly significant reduction of the infarct size in the CD34$^+$ and CD34$^+$KDR$^+$ cell groups, as compared with the PBS and CD34$^+$KDR$^-$ mice ($P<0.05$) (Fig. 4A, B).

Long-term effects on cardiac function

To determine whether the positive effects of CD34$^+$ cell injection on cardiac function were long- or short-lived, a number of mice injected with CD34$^+$ cells were analyzed at 5 months after induction of MI. As in the other experiments, +dP/dt, –dP/dt and LVEDP were evaluated. Results show a significant improvement of all parameters in mice injected with CD34$^+$ cells, as compared with PBS-injected control mice ($P < 0.05$) (Fig. 5), indicating that the therapeutic action of CD34$^+$ cells is maintained in the long term.

Histological analysis

Differentiation of CD34$^+$, CD34$^+$KDR$^+$, and CD34$^+$KDR$^-$ cells into endothelial and cardiac phenotypes

Fluorescence microscopy was used to investigate the incorporation of human CD34$^+$ cells transplanted in the peri-infarct area. Three weeks after MI, human cells were recognized in the NOD-SCID hearts using an antibody specific for human nuclear antigen (HNA). As shown in Fig. 6A, HNA$^+$ cells were detected in vessels of the cardiac muscle (red staining): these cells

stained positive also for lectin I (green color) in mice transplanted with CD34$^+$ cells, indicating the incorporation of human End progenitor cells into sites of neovascularization. Few CMCs stained with WGA (which stains for myocardial cell membranes, green staining) displayed also positivity for human nuclei (red staining) (see also figure legend). In the CD34$^+$ cell-injected group, we observed 3–13 cells positive for human nuclei/infarcted area (0.084 mm^2 × 3, ~75 cells per field). Specifically, we detected: (a) 0.32 ± 0.11 HNA$^+$/lectinI$^+$ cells per 100 analyzed vessels and (b) 7.0 ± 0.8 HNA$^+$/WGA$^+$ cells per 2000 analyzed fibers. Conversely, very few or no human positive cells were found in the MNCs and PBS-injected groups, respectively (data not shown). In hearts transplanted with CD34$^+$KDR$^+$ cells, we could detect HNA$^+$/Lectin I$^+$ cells (0.5±0.1%); the frequency of these double positive cells was significantly lower after transplantation of CD34$^+$KDR$^-$ cells (0.2±0.1%, P<0.05). (Fig. 6B). We also observed HNA$^+$/WGA$^+$ cells in CD34$^+$KDR$^+$ injected hearts (10±0.5), as compared with a significantly lower number in CD34$^+$KDR$^-$ injected hearts (6±0.6, P<0.05) (data not shown).

These findings indicate that CD34$^+$ cells and CD34$^+$KDR$^+$ cells transplanted into the peri-infarct area of NOD-SCID mice may contribute to neovascularization and differentiate into mature End cells and CMCs. The detection of rare human End or myocardial cells in the peri-infarct area of CD34$^+$KDR$^-$-injected hearts may partially be related to the purity of the CD34$^+$KDR$^-$ cell fraction, which may occasionally contain a few contaminating KDR$^+$ cells after cell sorting.

Effect of CD34$^+$ cell injection on myocardial fibrosis and cardiomyocyte apoptosis

Myocardial fibrosis is considered an indirect index of myocardial necrosis. Similarly, apoptosis is involved in the generation of heart failure in a number of different pathophysiological conditions. During acute myocardial ischemia, both fibrosis and apoptosis occur and are two important biological determinants of the alteration of cardiac function. It has been previously shown that cardiomyocyte apoptosis is greatly decreased in immunodepressed animals with myocardial ischemia after injection with human CD34$^+$ cells (5). Results from our experiments show a remarkable decrease of both myocardial fibrosis (Fig. 7A) and cardiomyocyte and noncardiomyocyte apoptosis in CD34$^+$ cell-injected mice (Fig. 7B).

CD34$^+$ and CD34$^+$KDR$^+$ cells can differentiate into CMCs by in vitro coculture assays

The experiments described in the previous section demonstrated that CMC differentiation in vivo from CB CD34$^+$ cells is a low-efficiency phenomenon. Whether human nuclear positivity within a CMC context is due to transdifferentiation rather than to cell fusion could not be established. We therefore conducted in vitro coculture studies aiming to determine whether cardiomyogenic differentiation could be obtained at an efficiency higher than that observed in vivo.

Therefore, CD34$^+$ cells, either untreated or expressing GFP, were cocultured with rat CMCs for 12–14 days in CMC medium. Cultures were then analyzed by immunofluorescence. Myocardial differentiation of human cells was demonstrated by cardiac Troponin I positivity, together with HNA and GFP positivity. As shown in Fig. 8A, GFP$^+$/HNA$^+$/Troponin I$^+$ cells represented 1–3% of the total number of cells at the end of a representative in vitro differentiation assay. Similar results were obtained with cells not prelabeled with GFP virus, in which the human origin was assessed only by HNA positivity (Fig. 8B). Approximately half of the cells were binucleated.

To investigate to which extent the trandsdifferentiative potential of CD34$^+$ cells is retained in the CD34$^+$KDR$^+$ fraction, we performed coculture experiments with the CD34$^+$KDR$^+$ subset in comparison with the CD34$^+$KDR$^-$ fraction. As shown in Fig. 9, in the CD34$^+$KDR$^+$ cell cocultures we could easily detect HNA$^+$ human cells with the typical myosin pattern of CMCs. Conversely, in the CD34$^+$KDR$^-$ cell cocultures, we could never detect HNA$^+$ human cells with a CMC myosin pattern, because the cells always maintained the characteristic round shape of hematopoietic cells. Furthermore, human CMCs were never observed in CD34$^+$KDR$^-$ cell cocultures up to a seeding density 100 times higher than that of CD34$^+$KDR$^+$ cells. Similar results were obtained upon cardiac troponin I staining (not shown).

DISCUSSION

We describe here the beneficial effects on cardiac function of human CB CD34$^+$ cells transplanted after MI in the NOD-SCID mouse model. This effect is demonstrated by invasive hemodynamic techniques. Moreover, we show that a small subfraction of these cells, the CD34$^+$KDR$^+$ subset, is endowed with a marked therapeutic potential, as its beneficial effect on hemodynamic parameters compares with that observed after transplantation of a two log higher number of CD34$^+$ cells. The therapeutic effect of low-dose CD34$^+$KDR$^+$ cells has been observed not only in the heart infarct (this manuscript) but also in the hind limb ischemia model (submitted manuscript). Since the CD34$^+$KDR$^+$ subset constitutes ~1% of CD34$^+$ cells, the results suggest that CD34$^+$KDR$^+$ cells represent the therapeutically active subfraction within the CD34$^+$ cell population. Accordingly, the CD34$^+$KDR$^-$ subset exerts little or no beneficial effect.

We show here that human CD34$^+$ cells are able to convert into CMCs in vivo, although with limited efficiency. Because of the low number of HNA$^+$ nuclei within a CMC context, we cannot rule out the possibility that the few CMCs newly formed in the transplanted heart are generated by cell fusion, as suggested (23). This mechanism cannot be ruled out in our in vitro coculture assays, which suggest that CMCs may be generated from both CD34$^+$ and CD34$^+$KDR$^+$ cells.

In our hands, the number of CMCs newly formed in vivo from CD34$^+$ cells is at least two log lower than previously reported in a syngeneic murine model transplanted with primitive hematopoietic cells (10). In the human transplanted hearts, it has been demonstrated that CMCs can be generated from BM stem cells (24), although conflicting data exist on the extent of this phenomenon. In fact, in subsequent reports, the number of newly formed CMCs from BM stem cells in transplanted patients was much lower (25, 26). Similarly, the BM cell subset isolated through Hoechst staining uptake ("side-population"), transplanted into irradiated NOD-SCID mice, was endowed with neocardiomyogenic potential, but only at a limited extent (12, 23). In line with these findings, the results presented here suggest that CD34$^+$KDR$^+$ Hem-End primitive cells have cardiomyogenic potential at a limited extent.

We have previously shown that End progenitor cells with hematopoietic potential from the murine embryonic dorsal aorta, as well as HUVEC cells, are able to differentiate in CMCs in coculture experiments (13). More recently, it has been shown that human End progenitor cells from PB were also able to differentiate into CMCs in coculture assays (14). In our studies, the fraction of CD34$^+$ cells from CB differentiating toward angiogenesis and cardiomyogenesis is apparently represented by the CD34$^+$KDR$^+$ subfraction: This cell subset, enriched for End

progenitors and hemangioblasts (16, 17), might be related to the End precursor populations reportedly endowed with cardiomyogenic potential (14).

CD34$^+$ and CD34$^+$KDR$^+$ CB cells, while of limited cardiomyogenic potential, have a marked angiogenetic capacity: This provides hope for a therapeutic use of these cells in chronic ischemic disorders. The angiogenic potential is in fact elevated, as shown by the low level of both fibrosis and CMC apoptosis in the myocardium of mice receiving an injection of CD34$^+$ or CD34$^+$KDR$^+$ cells. Similarly, a decrease in cardiomyocyte apoptosis linked to an improvement of cardiac function was obtained by injection in the tail vein of human PB CD34$^+$ cells after MI in immunodepressed rats (5). Noteworthily, in our model a low number of MNCs were not able to induce angiogenesis and improve heart function, as previously reported using a large number of MNCs (3) or End cells ex vivo expanded from BM MNCs (2, 4, 6).

The therapeutic efficacy of a small number of CD34$^+$KDR$^+$ cells is a novel and important finding, seemingly mediated by diverse factors. 1) As mentioned above, the CD34$^+$KDR$^+$ subfraction is not only enriched for Hem and End progenitor/stem cells, but also comprises hemangioblasts, that is, cells with the capacity to generate both Hem and End progeny (15–17). Single-cell culture studies indicate that these functionally different cell populations may represent a single cell pool exhibiting hematopoietic and/or endothelial differentiation in different microenvironmental conditions (16). In the MI model used here, the transplanted CD34$^+$KDR$^+$ cells may be channeled into End differentiation, and limited CMC generation. 2) CD34$^+$KDR$^+$ cells are exquisitely resistant to apoptosis in serum-free GF-starved culture via autocrine VEGF release (see also 22); conversely, CD34$^+$KDR$^-$ cells rapidly die in these harsh culture conditions. We suggest, therefore, that CD34$^+$KDR$^+$ (but not KDR$^-$) cells may be particularly resistant to apoptosis when transplanted in the heart infarct area: Ongoing studies aim to verify this aspect. 3) The small number of transplanted CD34$^+$KDR$^+$ cells, releasing significant amounts of VEGF, may exert an antiapoptotic and proliferative action on murine heart ECs, thus enhancing capillarization and improving survival of CMCs. Hypothetically, CD34$^+$KDR$^+$ cells may activate cardiac stem cells and/or release factors exerting a direct antiapoptotic effect on CMCs: preliminary coculture studies suggest in fact a direct antiapoptotic action.

Altogether, our results indicate that, within the CD34$^+$ cell population, the CD34$^+$KDR$^+$ fraction is responsible for the improvement in cardiac hemodynamics, and, hence, represents the candidate active CD34$^+$ cell subset. Admittedly, the number of available CD34$^+$KDR$^+$ cells is limited. In this regard, ongoing studies in our laboratory aim to expand ex vivo the CD34$^+$KDR$^+$ subset, in order to facilitate its therapeutic use at preclinical and then possibly clinical levels.

ACKNOWLEDGMENTS

REFERENCES

1. Isner, J. M., and Asahara, T. (1999) Angiogenesis and vasculogenesis as therapeutic strategies for postnatal neovascularization. *J. Clin. Invest.* **103**, 1231–1236

2. Kalka, C., Masuda, H., Takahashi, T., Kalka-Moll, W. M., Silver, M., Kearney, M., Li, T., Isner, J. M., and Asahara, T. (2000) Transplantation of ex vivo expanded endothelial progenitor cells for therapeutic neovascularization. *Proc. Natl. Acad. Sci. U.S.A.* **97**, 3422–3427

3. Kamihata, H., Matsubara, H., Nishiue, T., Fujiyama, S., Tsutsumi, Y., Ozono, R., Masaki, H., Mori, Y., Iba, O., Tateishi, E., et al. (2001) Implantation of bone marrow mononuclear cells into ischemic myocardium enhances collateral perfusion and regional function via side supply of angioblasts, angiogenic ligands, and cytokines. *Circulation* **104**, 1046–1052

4. Kawamoto, A., Gwon, H. C., Iwaguro, H., Yamaguchi, J. I., Uchida, S., Masuda, H., Silver, M., Ma, H., Kearney, M., Isner, J. M., et al. (2001) Therapeutic potential of ex vivo expanded endothelial progenitor cells for myocardial ischemia. *Circulation* **103**, 634–637

5. Kocher, A. A., Schuster, M. D., Szabolcs, M. J., Takuma, S., Burkhoff, D., Wang, J., Homma, S., Edwards, N. M., and Itescu, S. (2001) Neovascularization of ischemic myocardium by human bone-marrow-derived angioblasts prevents cardiomyocyte apoptosis, reduces remodeling and improves cardiac function. *Nat. Med.* **7**, 430–436

6. Kawamoto, A., Tkebuchava, T., Yamaguchi, J., Nishimura, H., Yoon, Y. S., Milliken, C., Uchida, S., Masuo, O., Iwaguro, H., Ma, H., et al. (2003) Intramyocardial transplantation of autologous endothelial progenitor cells for therapeutic neovascularization of myocardial ischemia. *Circulation* **107**, 461–468

7. Strauer, B. E., Brehm, M., Zeus, T., Kostering, M., Hernandez, A., Sorg, R. V., Kogler, G., and Wernet, P. (2002) Repair of infarcted myocardium by autologous intracoronary mononuclear bone marrow cell transplantation in humans. *Circulation* **106**, 1913–1918

8. Assmus, B., Schachinger, V., Teupe, C., Britten, M., Lehmann, R., Dobert, N., Grunwald, F., Aicher, A., Urbich, C., Martin, H., et al. (2002) Transplantation of progenitor cells and regeneration enhancement in acute myocardial infarction (TOPCARE-AMI). *Circulation* **106**, 3009–3017

9. Asahara, T., Murohara, T., Sullivan, A., Silver, M., van der Zee, R., Li, T., Witzenbichler, B., Schatteman, G., and Isner, J. M. (1997) Isolation of putative progenitor endothelial cells for angiogenesis. *Science* **275**, 964–967

10. Orlic, D., Kajstura, J., Chimenti, S., Jakoniuk, I., Anderson, S. M., Li, B., Pickel, J., McKay, R., Nadal-Ginard, B., Bodine, D. M., et al. (2001) Bone marrow cells regenerate infarcted myocardium. *Nature* **410**, 701–705

11. Orlic, D., Kajstura, J., Chimenti, S., Limana, F., Jakoniuk, I., Quaini, F., Nadal-Ginard, B., Bodine, D. M., Leri, A., and Anversa, P. (2001) Mobilized bone marrow cells repair the

infarcted heart, improving function and survival. *Proc. Natl. Acad. Sci. U.S.A.* **98**, 10,344–10,349

12. Jackson, K. A., Majka, S. M., Wang, H., Pocius, J., Hartley, C. J., Majesky, M. W., Entman, M. L., Michael, L. H., Hirschi, K. K., and Goodell, M. A. (2001) Regeneration of ischemic cardiac muscle and vascular endothelium by adult stem cells. *J. Clin. Invest.* **107**, 1395–1402

13. Condorelli, G., Borello, U., De Angelis, L., Latronico, M., Sirabella, D., Coletta, M., Galli, R., Balconi, G., Follenzi, A., Frati, G., et al. (2001) Cardiomyocytes induce endothelial cells to trans-differentiate into cardiac muscle: Implications for myocardium regeneration. *Proc. Natl. Acad. Sci. U.S.A.* **98**, 10,733–10,738

14. Badorff, C., Brandes, R. P., Popp, R., Rupp, S., Urbich, C., Aicher, A., Fleming, I., Busse, R., Zeiher, A. M., and Dimmeler, S. (2003) Transdifferentiation of blood-derived human adult endothelial progenitor cells into functionally active cardiomyocytes. *Circulation* **107**, 1024–1032

15. Ziegler, B. L., Valtieri, M., Porada, G. A., De Maria, R., Muller, R., Masella, B., Gabbianelli, M., Casella, I., Pelosi, E., Bock, T., et al. (1999) KDR receptor: A key marker defining hematopoietic stem cells. *Science* **285**, 1553–1558

16. Pelosi, E., Valtieri, M., Coppola, S., Botta, R., Gabbianelli, M., Lulli, V., Marziali, G., Masella, B., Muller, R., Sgadari, C., et al. (2002) Identification of the hemangioblast in postnatal life. *Blood* **100**, 3203–3208

17. Peichev, M., Naiyer, A. J., Pereira, D., Zhu, Z., Lane, W. J., Williams, M., Oz, M. C., Hicklin, D. J., Witte, L., Moore, M. A., et al. (2000) Expression of VEGFR-2 and AC133 by circulating human CD34^{+} cells identifies a population of functional endothelial precursors. *Blood* **95**, 952–958

18. Bonci, D., Cittadini, A., Latronico, M., Borello, U., Aycock, J. K., Drusco, A., Innocenzi, A., Follenzi, A., Lavitrano, M. L., Monti, M. G., et al. (2003) Advanced generation lentiviruses as efficient vectors for cardiomyocyte gene transduction in vitro and in vivo. *Gene Ther.* **10**, 630–636

19. Condorelli, G., Roncarati, R., Ross, J., Jr., Pisani, A., Stassi, G., Todaro, M., Trocha, S., Drusco, A., Gu, Y., Russo, M. A., et al. (2001) Heart-targeted overexpression of caspase3 in mice increases infarct size and depresses cardiac function. *Proc. Natl. Acad. Sci. U.S.A.* **98**, 9977–9982

20. Tsuda, T., Gao, E., Evangelisti, L., Markova, D., Ma, X., and Chu, M.-L. (2003) Post-ischemic myocardial fibrosis occurs independent of hemodynamic changes. *Cardiovasc. Res.* **59**, 926–933

21. Condorelli, G. L., Morisco, C., Stassi, G., Roncarati, R., Farina, F., Trimarco, B., and Lembo, G. (1999) Increased cardiomyocyte apoptosis and changes in proapoptotic and

antiapoptotic genes bax and bcl-2 during left ventricular adaptations to chronic pressure overload in the rat. *Circulation* **23,** 3071–3078

22. Gerber, H. P., Malik, A. K., Solar, G. P., Sherman, D., Liang, X. H., Meng, G., Hong, K., Marsters, J. C., and Ferrara, N. (2002) VEGF regulates haematopoietic stem cell survival by an internal autocrine loop mechanism. *Nature* **417,** 954–958

23. Alvarez-Dolado, M., Pardal, R., Garcia-Verdugo, J. M., Fike, J. R., Lee, H. O., Pfeffer, K., Lois, C., Morrison, S. J., and Alvarez-Buylla, A. (2003) Fusion of bone-marrow-derived cells with Purkinje neurons, cardiomyocytes, and hepatocytes. *Nature* **425,** 968–973

24. Quaini, F., Urbanek, K., Beltrami, A. P., Finato, N., Beltrami, C. A., Nadal-Ginard, B., Kajstura, J., Leri, A., and Anversa, P. (2002) Chimerism of the transplanted heart. *N. Engl. J. Med.* **346,** 5–15

25. Laflamme, M. A., Myerson, D., Saffitz, J. E., and Murry, C. E. (2002) Evidence for cardiomyocyte repopulation by extracardiac progenitors in transplanted human hearts. *Circ. Res.* **90,** 634–640

26. Deb, A., Wang, S., Skelding, K. A., Miller, D., Simper, D., and Caplice, N. M. (2003) Bone marrow-derived cardiomyocytes are present in adult human heart: A study of gender-mismatched bone marrow transplantation patients. *Circulation* **107,** 1247–1249

Table 1

VEGF released by CD34$^+$, CD34$^+$KDR$^+$ and CD34$^+$KDR$^-$ cells after 48 h in liquid suspension serum-free starvation culture

Cell type	Cell No./Volume	VEGF released in medium (pg/ml)*
None	0/0.2 ml FCS$^-$ medium	0
CD34$^+$	50 × 10^3/0.2 ml	50.0 ± 4.1
CD34$^+$KDR$^-$	50 × 10^3/0.2 ml	41.3 ± 12.6
CD34$^+$KDR$^+$	10^3/0.2 ml	42.5 ± 9.7

*Mean ± SEM values from four separate experiments.

Fig. 1
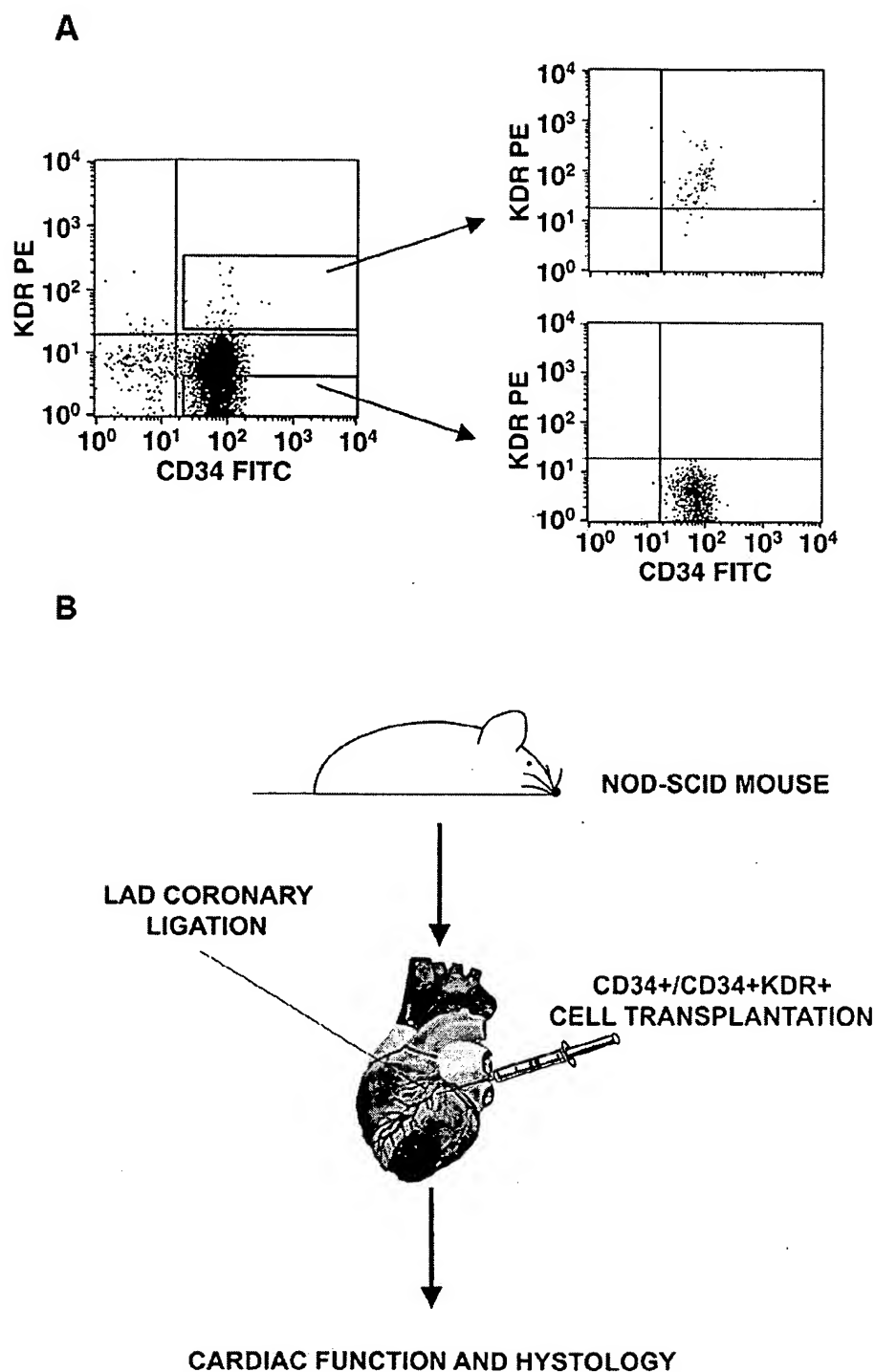
Figure 1. *A*) Human CB CD34⁺KDR⁺ cell purification. (*Left*) Representative FACS profile of CD34⁺ cells isolated from human CB and labeled with CD34-FITC and biotinylated KDR-PE antibody. (*Right*) Quality control reanalysis of the sorted CD34⁺KDR⁺ and CD34⁺KDR⁻ fractions. *B*) Experimental procedure. Schematic model of myocardial infarction (MI) in NOD-SCID mice by ligation of left anterior descending coronary artery.

Fig. 2
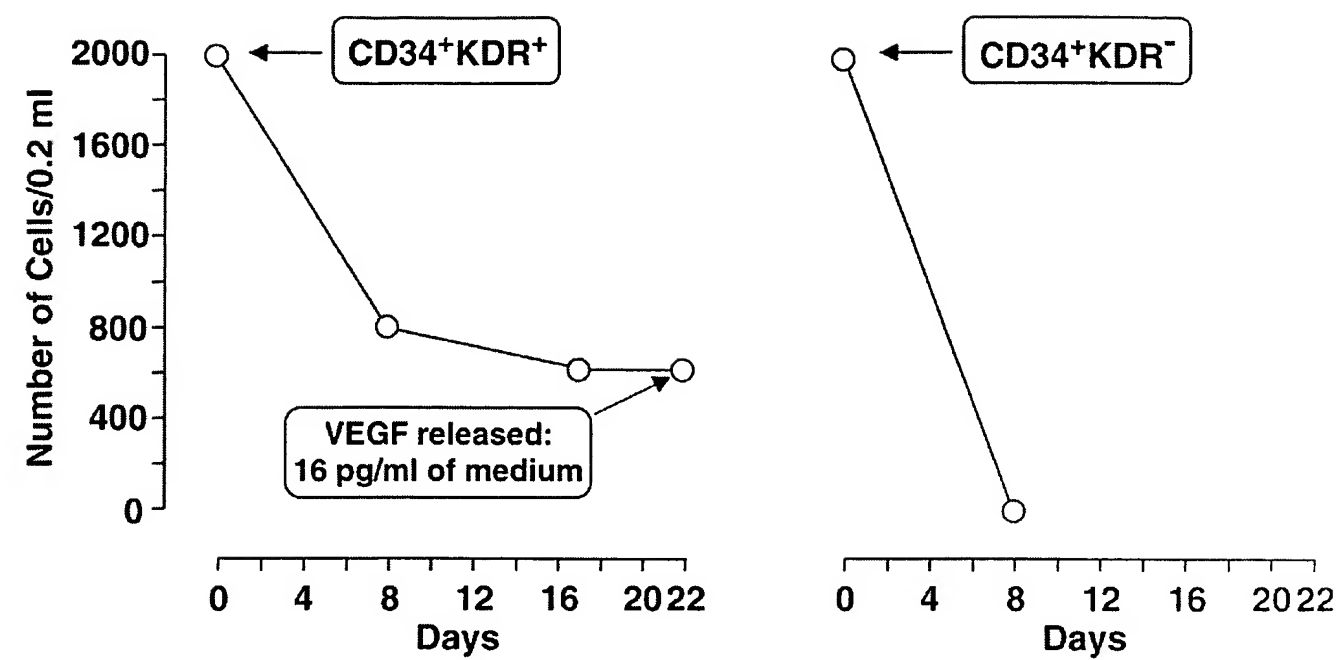
Figure 2. Resistance to apoptosis of CD34⁺KDR⁺ and CD34⁺KDR⁻ cells seeded at low number (2×10³ cells/0.2 ml) in U-shaped wells containing serum-free medium. Autocrine released VEGF is also indicated. A representative experiment is shown.

Fig. 3
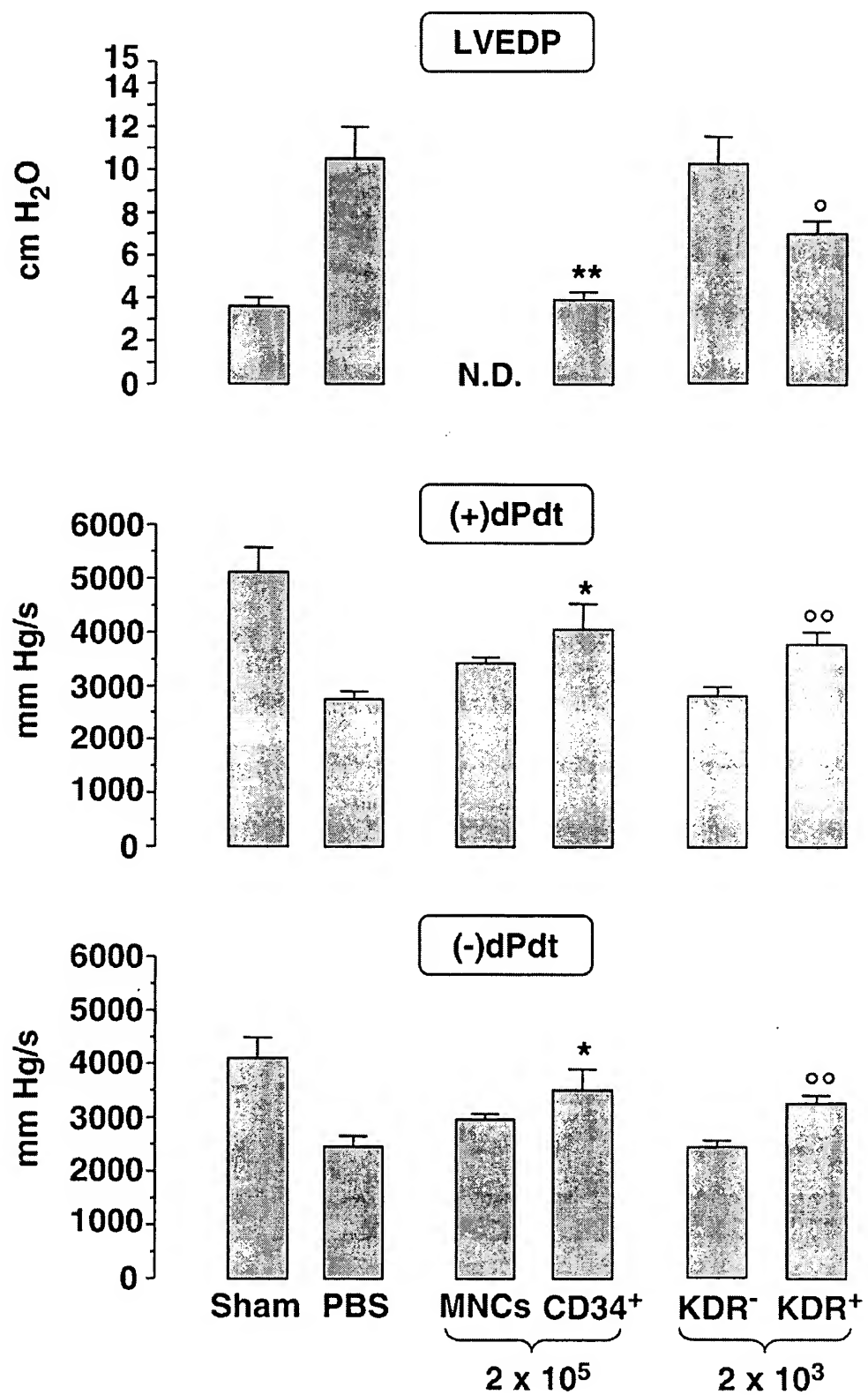
Figure 3. Hemodynamic effects of CB cell injection 3 weeks after MI in NOD-SCID mice. Hemodynamic parameters in mice injected with CD34$^+$ cells and MNCs (2×10^5cells), CD34$^+$KDR$^+$, and CD34$^+$KDR$^-$ (2×10^3cells) cells after MI, as compared with the Sham and PBS control groups. Analysis was performed 21 days after induction of myocardial infarction and cell transplantation. Mean ± SEM data from 4–9 animals per group are presented. (*upper panel*) Left Ventricular End Diastolic Pressure (LVEDP) evaluation: hearts injected with CD34$^+$KDR$^+$ cells showed significantly lower values than those injected with PBS or CD34$^+$KDR$^-$ cells ($^\circ P<0.05$), likewise CD34$^+$ vs. PBS-injected ($^{**}P<0.01$), N.D.: not done. (*middle panel*) Evaluation of the derivative of pressure over time (+dP/dt): CD34$^+$ and CD34$^+$KDR$^+$ groups showed significantly higher values, as compared with PBS control and CD34$^+$KDR$^-$ groups ($^*P<0.05$ for CD34$^+$ vs. PBS; $^{\circ\circ}P<0.01$ for CD34$^+$KDR$^+$ vs. PBS or CD34$^+$KDR$^-$). (*lower panel*) Evaluation of (−)dP/dt showed higher values for CD34$^+$ group as compared with PBS control ($^*P<0.05$) and for CD34$^+$KDR$^+$ cells vs. PBS or CD34$^+$KDR$^-$ groups ($^{\circ\circ}P<0.01$).

Fig. 4

A

Sham
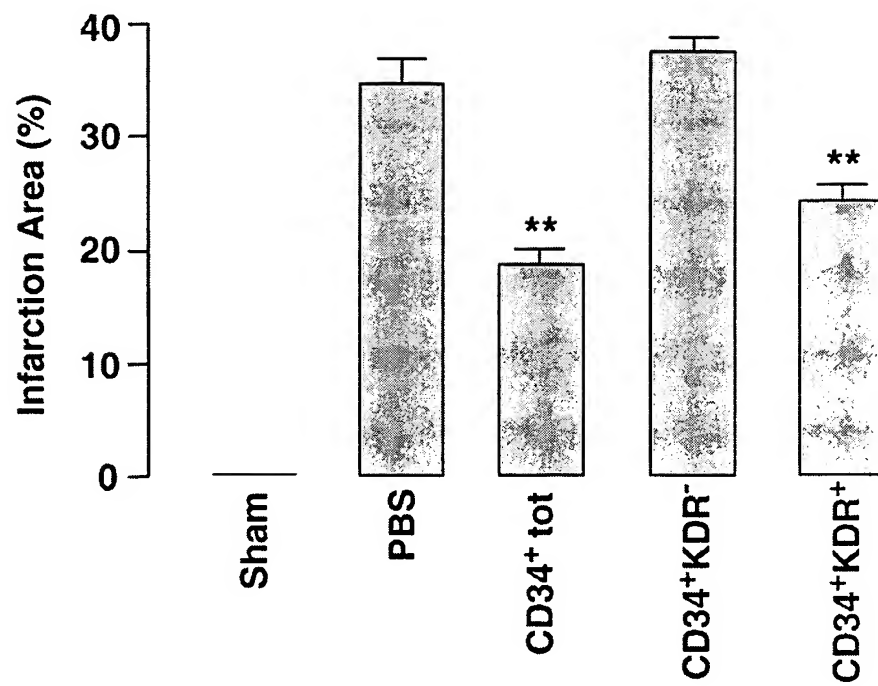
PBS

CD34$^+$ tot
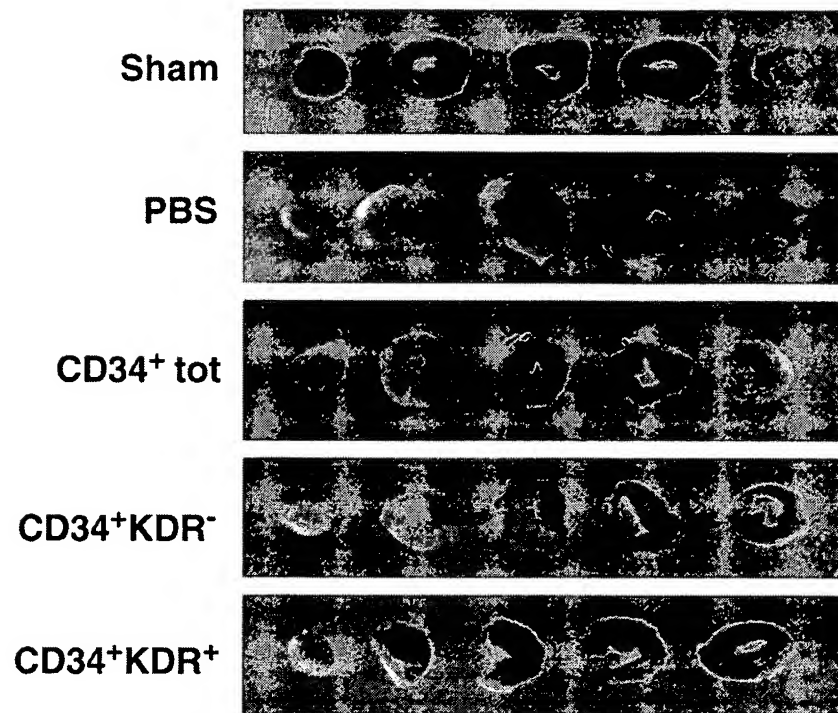
CD34$^+$KDR$^-$

CD34$^+$KDR$^+$

B

Figure 4. Extension of the infarct area in NOD-SCID mice injected with unseparated CD34$^+$ or CD34$^+$KDR$^+$ cells as compared with PBS- or CD34$^+$KDR- injected mice 3 weeks after MI. *A*) Representative TTC staining in hearts from mice transplanted with CD34$^+$, CD34$^+$KDR$^+$, or CD34$^+$KDR$^-$ cells or injected with PBS after MI, as compared with Sham control. *B*) Size of infarction area at 21 days after MI in mice injected with CD34$^+$ cells (*n*=6), CD34$^+$KDR$^+$ or CD34$^+$KDR$^-$ cells (*n*=4), PBS (*n*=8) or Sham control mouse. Infarction area is expressed as percentage of necrotic tissue by TTC staining. Mean ± SEM values are presented. **P<0.01 vs. PBS and KDR$^-$ group.

Fig. 5
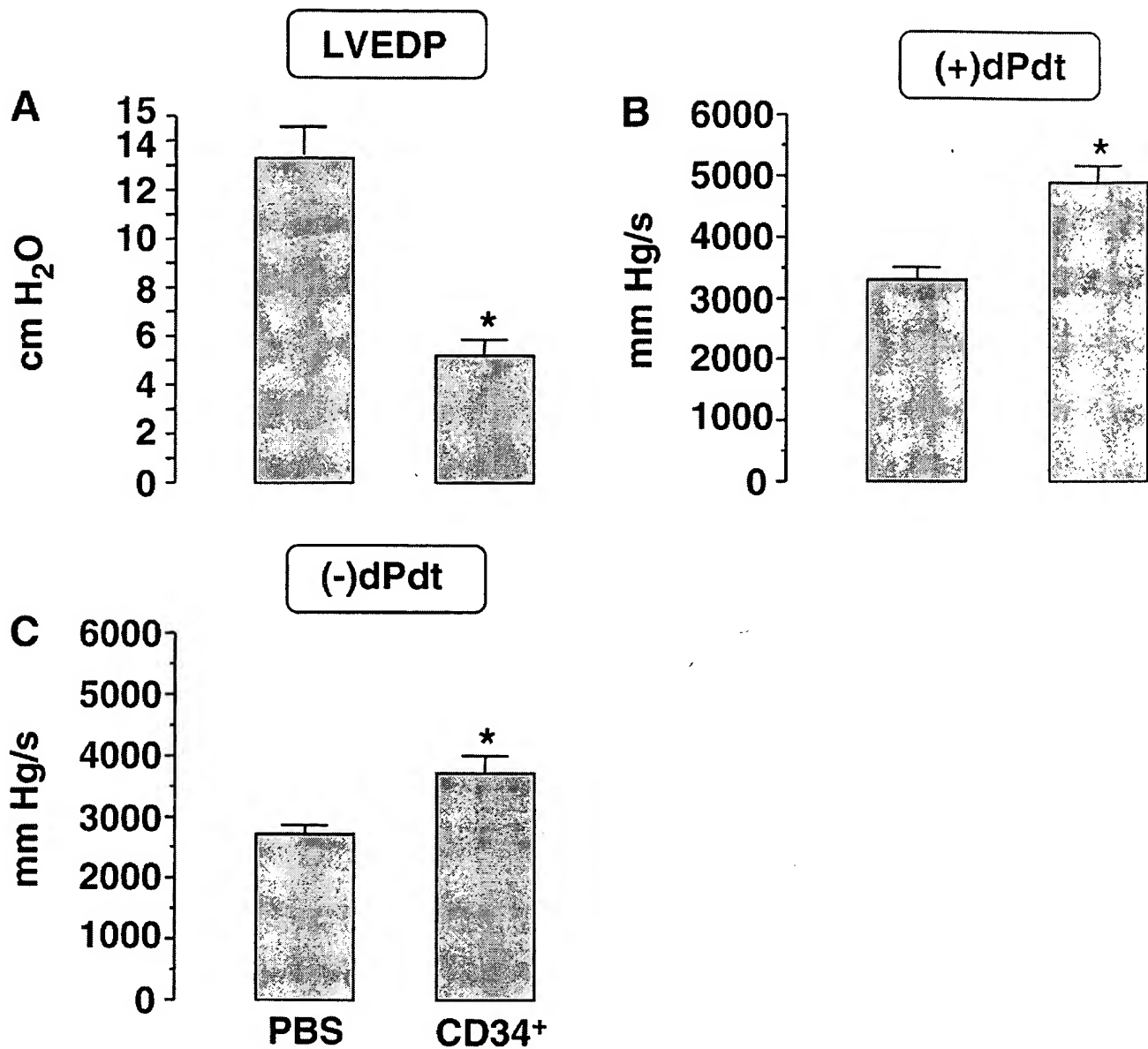
Figure 5. Hemodynamic effects of CD34$^+$ injection 5 months after MI in NOD-SCID mice. *A*) Evaluation of Left Ventricular End Diastolic Pressure (LVEDP). Hearts injected with CD34$^+$ cells after MI showed significantly lower values (*$P<0.05$) than those injected with PBS. *B*) Evaluation of the derivative of pressure over time (+dP/dt): CD34$^+$ group showed significant higher values as compared with the PBS control group (*$P<0.05$). *C*) Evaluation of (–)dP/dt showed significant higher values for CD34$^+$ group as compared with the PBS group, (*$P<0.05$).

Fig. 6

A

WGA **LECTIN**

Normal Control

PBS

CD34+

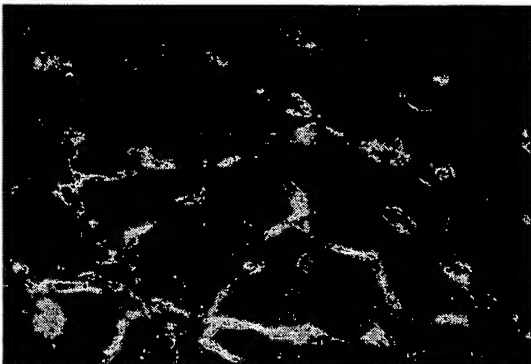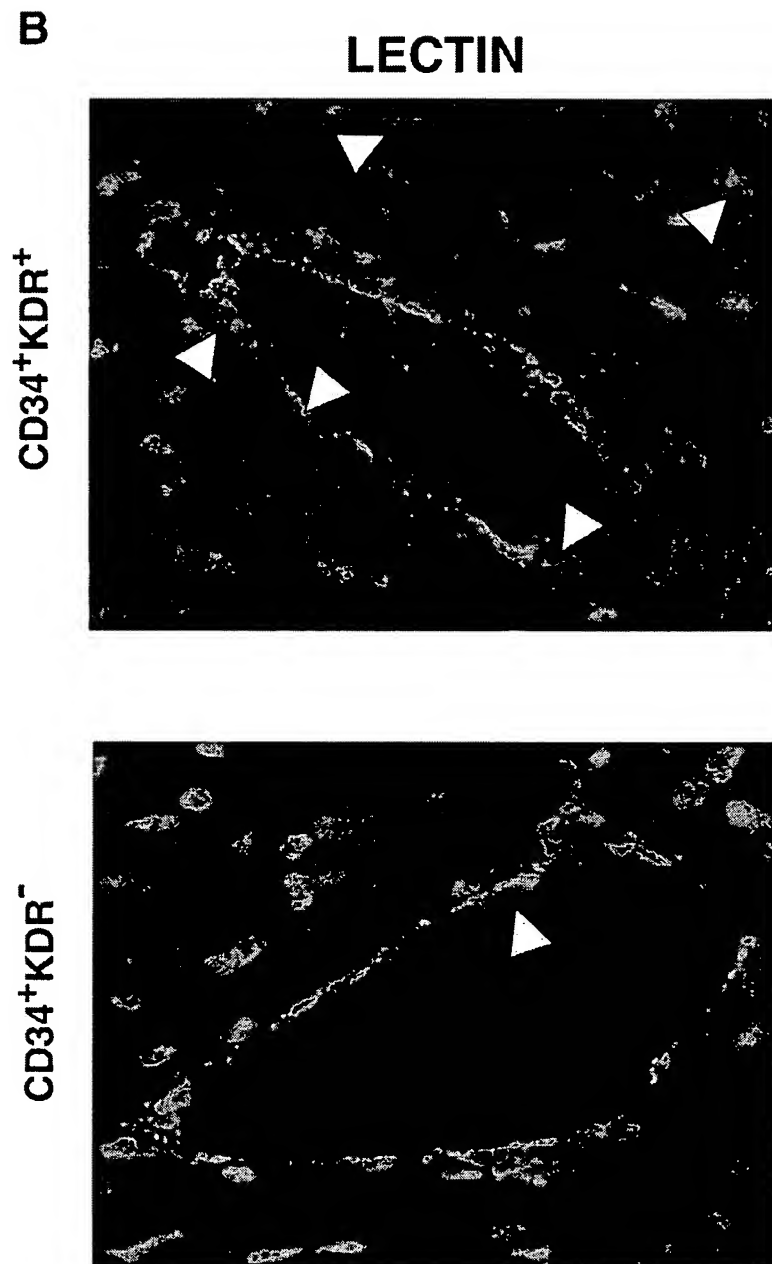Fig. 6 (cont)

B

LECTIN
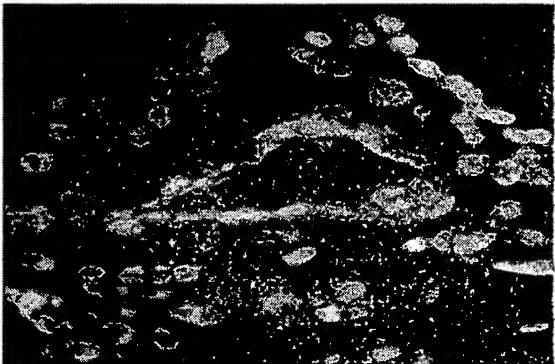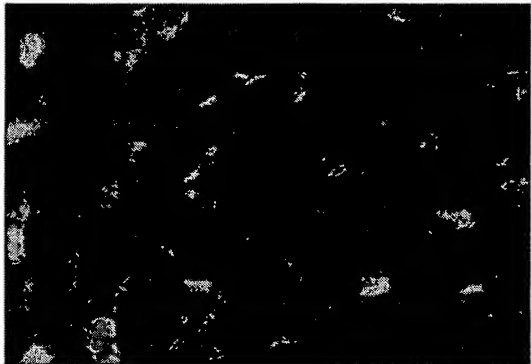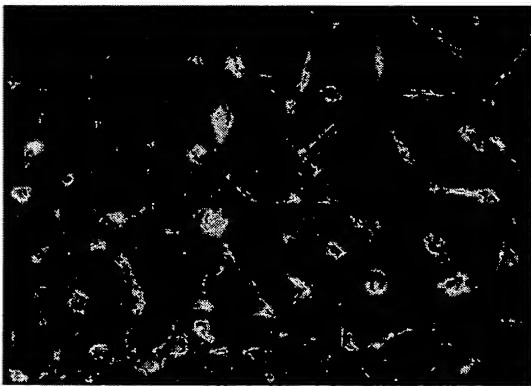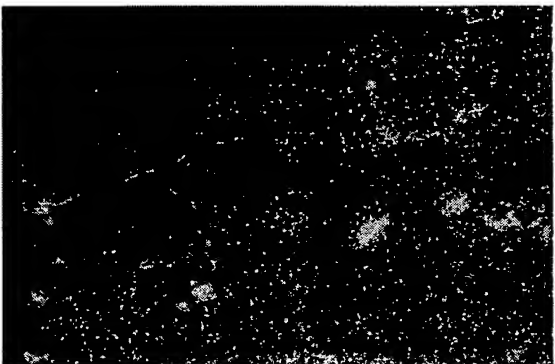
Figure 6. Myocardial and endothelial differentiation in the postischemic heart of NOD-SCID mice injected with CD34$^+$ or CD34$^+$KDR$^+$ cells. *A*) Samples are triple stained for nuclear Hoechst (blue color), human nuclear antigen (HNA, red) and WGA staining for cell membranes (green, *left panels*) or Lectin staining for endothelial cell membranes (green, *right panels*). Upper panels: Hoechst, HNA and WGA or Lectin staining of normal human myocardial tissue (positive control). Middle panels: Hoechst, HNA and WGA or Lectin staining of myocardial tissue from PBS-injected mice (negative control). Lower panels: Hoechst, HNA and WGA or Lectin staining of myocardial tissue isolated from CB CD34$^+$ transplanted mice. *B*) Hoechst, HNA and Lectin staining of myocardial tissue isolated from CD34$^+$KDR$^+$ (*upper panel*) and CD34$^+$KDR$^-$ (*lower panel*) transplanted mice. Arrows indicate HNA$^+$ cells.

Fig. 7

A

PBS

CD34⁺
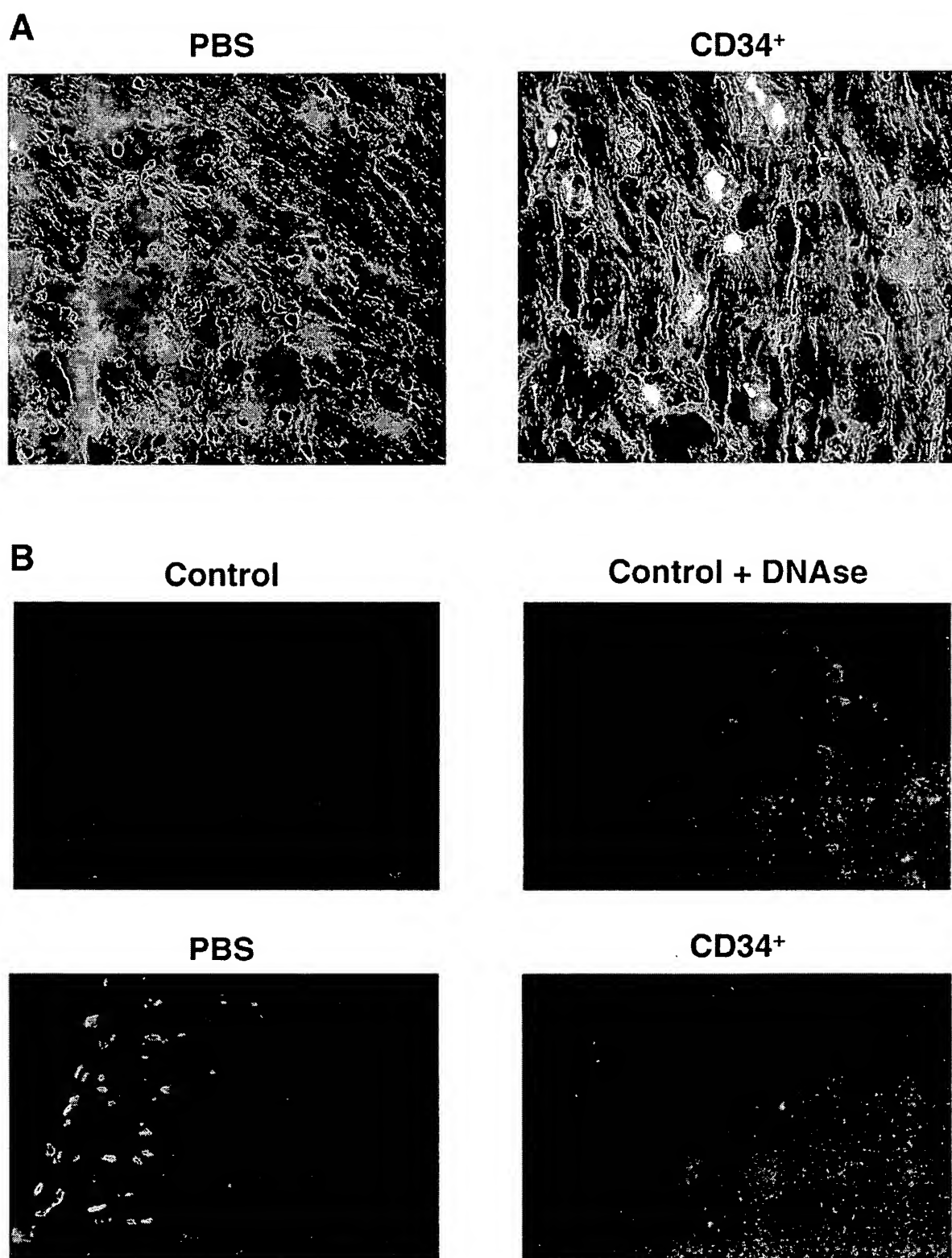

B

Control

Control + DNAse

PBS

CD34⁺

Figure 7. **Assessment of fibrosis and apoptosis in CD34⁺ vs. PBS-injected mice after MI.** *A*) Masson three chromic staining of myocardial tissue isolated from mice injected with PBS (*left panel*) or CD34⁺ cells (*right panel*). *B*) Tunel (green) and phalloidin (red) staining in nonischemic NOD-SCID mouse myocardium (negative control, *upper left*), DNAse-treated mouse myocardium (positive control, *upper right*), NOD-SCID mouse myocardium injected with PBS after MI (*lower left*), or with CD34⁺ cells (*lower right*).
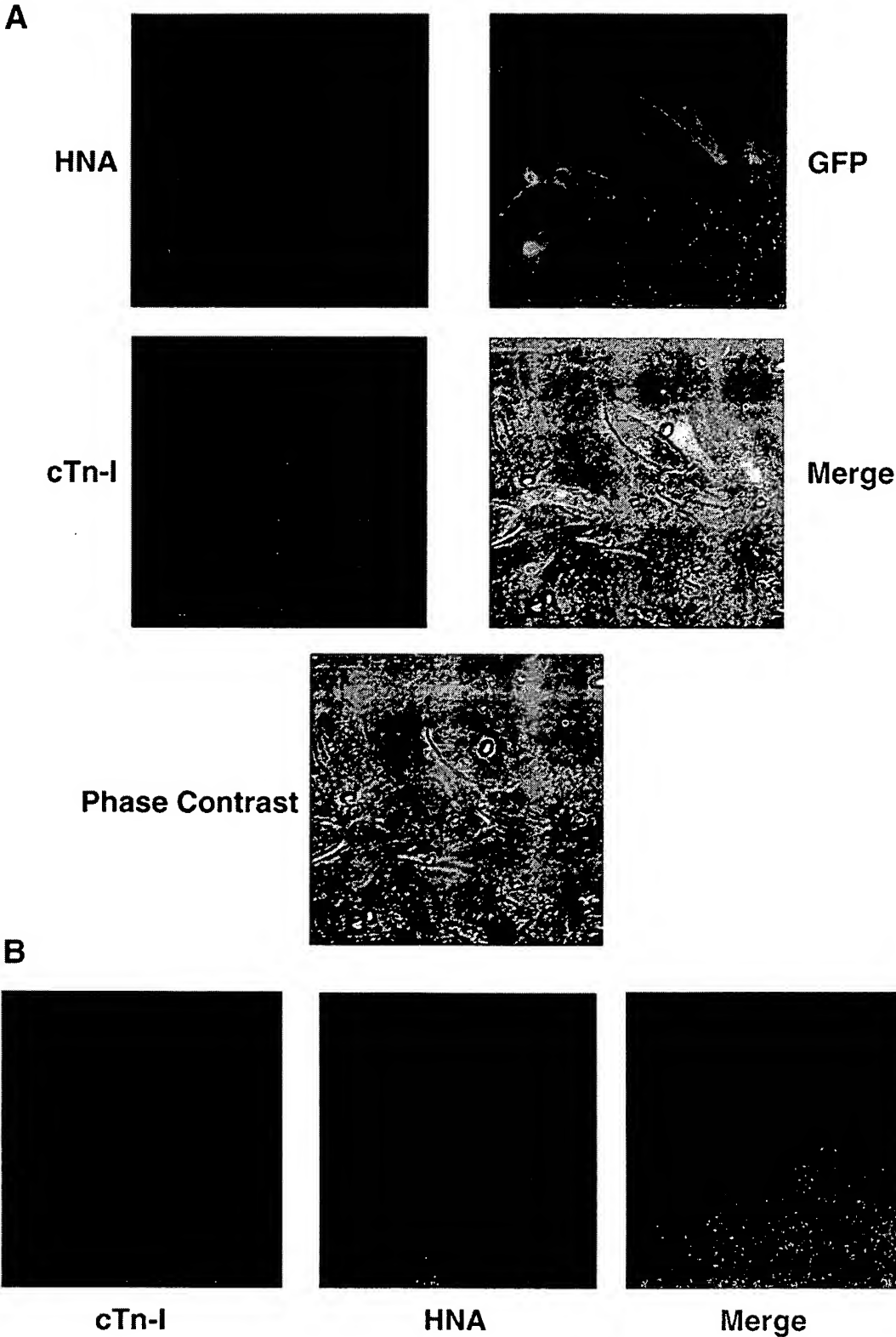
Fig. 8

A

HNA

GFP

cTn-I

Merge

Phase Contrast

B

cTn-I

HNA

Merge

Figure 8. In vitro coculture of CD34⁺ cells with rat CMCs. CD34⁺ cells were cocultured with 10^5 rat neonatal CMCs for 14 days; immunofluorescence for HNA (red) and α-cardiac Troponin-I (blue) was then performed. Confocal images with 40× original magnification. *A*) 5×10^3 CD34⁺/GFP⁺ were seeded in cocultures. (*upper left*) HNA. (*upper right*) GFP. (*middle left*) Cardiac Troponin I. (*middle right*) Merge. (*lower panel*) Phase contrast. *B*) 1×10^4 CD34⁺ cells were seeded in cocultures. (*left panel*) Cardiac Troponin I; (*middle*) HNA; (*right*) merge.
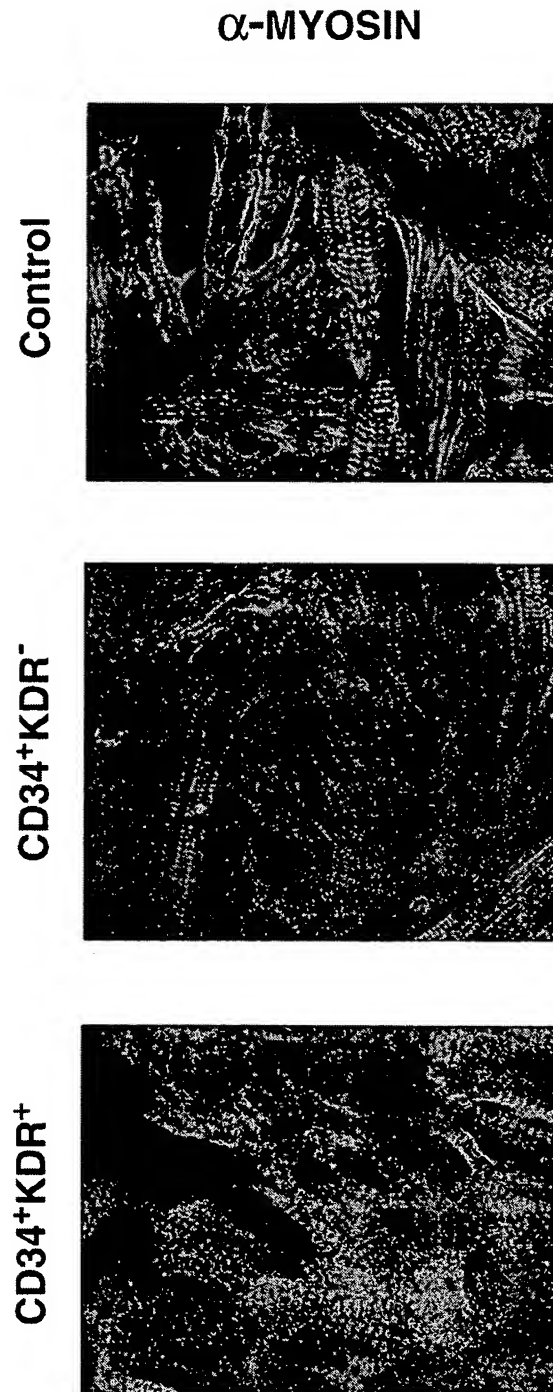
Fig. 9

α-MYOSIN

Figure 9. In vitro coculture of human CD34⁺KDR⁺ and CD34⁺KDR⁻ cells with rat CMCs. 3×10^3 CD34⁺KDR⁺ and CD34⁺KDR⁻ cells were cocultured with rat neonatal CMCs; after 14 days, immunofluorescence analysis for HNA (red) and α-myosin (green) was performed, followed by confocal microscopy (60×). (*upper panel*) Control rat CMCs. (*middle*) CD34⁺KDR⁻ cells. (*lower*) CD34⁺KDR⁺ cells.